TISSUE ENGINEERING: Part A
Volume 16, Number 4, 2010

DOI: 10.1089/ten.tea.2009.0404

Adipose-Derived Stem Cell Delivery into Collagen Gels Using Chitosan Microspheres

Shanmugasundaram Natesan, Ph.D.,[1] David G. Baer, Ph.D.,[1] Thomas J. Walters, Ph.D.,[1] Mary Babu, Ph.D.,[2] and Robert J. Christy, Ph.D.[1]

Integration of stem cells to injured tissues requires an appropriate delivery device and scaffolding system. In the present study we have developed an *in vitro* strategy to load and release adipose-derived mesenchymal stem cells (ASC) from chitosan microspheres (CSM) into a collagen gel scaffold. Porous CSM of uniform size and composition were prepared and used as a stem cell carrier. ASC were allowed to attach to the microspheres and infiltrate through the microsphere pores. The number of viable cells was counted *in vitro*, using MTT and Calcein acetoxymethyl ester (AM) assays, and it showed a proportional increase with seeding density and reached a maximum cell number by 24 h. The cells inside the microspheres remained metabolically active and viable, could be retrieved from the spheres, and maintained expression of stem-cell-specific markers. Electron microscopic evaluation of the cell–microsphere complex showed that the CSM were able to support cell attachment and that the cells had infiltrated into the pores of the microspheres. The ability of the cells to proliferate and differentiate into adipogenic- and osteogenic-like precursors indicates that the cells have maintained their multipotency after migration out of the microspheres. To mimic cell delivery into a tissue, ASC-loaded CSM were embedded in type-1 collagen scaffold by mixing them with type-1 collagen solution while inducing gelation. By 14 days the cells released into the collagen gel and were able to populate the entire scaffold. When observed through transmission electron microscopy, the cells align along the collagen fibrils with a characteristic fibroblast-like morphology. This study provides a model to capture pluripotent stem cells, expand their cell number within a biomaterial scaffold *in vitro*, and deliver within an appropriate matrix to repair damaged tissue.

Introduction

Regenerative therapies using stem-cell-based tissue engineering approaches offer the potential for the treatment of diseases, as well as the repair of damaged tissue and organs.[1–3] Adult mesenchymal stem cells are a population of fibroblast-like progenitor cells that possess a capacity of self-renewal, long-term viability, and multiple lineage potential.[4] Mesenchymal stem cells derived from adipose tissues (ASC) differentiate into multiple phenotypes, including adipose, muscle, bone, neuronal, endothelial, hepatocyte, and epithelial-like cells.[5–9] ASC are easily isolated from the stromal vasculature of subcutaneous adipose tissue by liposuction with minimally invasive procedures, and the excised adipose contains 100–1000 times more pluripotent cells per cubic centimeter than bone marrow.[10] This makes adipose tissue an attractive *in vivo* cellular source of autologous stem cells for regenerative therapies. Recent studies provide evidence that ASC expanded *in vitro* lack cellular immunogenicity and are nonimmunogenic even when used in immunocompetent animals.[11,12] Other immunological data provide evidence that ASC do not stimulate alloreactivity and were found to exhibit immunosuppressive activity, suggesting that ASC can be transplanted safely.[13–15] ASC when delivered to tissue defects elicit tissue regeneration by paracrine activation of host cells through secretion of growth factors,[16,17] autocrine signaling,[18] or through direct cell–cell interactions.[19,20]

Cell-based therapies to repair and regenerate tissues have tremendous potential to treat a wide array of tissue defects and diseases.[21–23] Current tissue engineering techniques implant stem cells directly, use aqueous solutions including saline or plasma[24,25] as carrier, or deliver cells in a three-dimensional (3D) biocompatible and biodegradable matrix to replace the specific injured tissue.[26] Still, a major challenge remains in the repair of large soft-tissue trauma that predominate in combat-related extremity injuries. These injuries are normally large and usually involve multiple tissue types, including skin, muscle, tendon, and bone, that need to be repaired.[27] Scaffold materials provide stem cells an environment favorable for adhesion, proliferation, and differentiation

[1]Regenerative Medicine Research Program, United States Army Institute of Surgical Research, Fort Sam Houston, Texas.
[2]Central Leather Research Institute, Ticel Biopark, Chennai, India.

Report Documentation Page

Form Approved
OMB No. 0704-0188

1. REPORT DATE	2. REPORT TYPE	3. DATES COVERED
01 APR 2010	**N/A**	**-**

4. TITLE AND SUBTITLE	5a. CONTRACT NUMBER
Adipose-derived stem cell delivery into collagen gels using chitosan microspheres	5b. GRANT NUMBER
	5c. PROGRAM ELEMENT NUMBER
6. AUTHOR(S)	5d. PROJECT NUMBER
Natesan S., Baer D. G., Walters T. J., Babu M., Christy R. J.,	5e. TASK NUMBER
	5f. WORK UNIT NUMBER
7. PERFORMING ORGANIZATION NAME(S) AND ADDRESS(ES)	8. PERFORMING ORGANIZATION REPORT NUMBER
United States Army Institute of Surgical Research, JBSA Fort Sam Houston, TX 78234	
9. SPONSORING/MONITORING AGENCY NAME(S) AND ADDRESS(ES)	10. SPONSOR/MONITOR'S ACRONYM(S)
	11. SPONSOR/MONITOR'S REPORT NUMBER(S)

12. DISTRIBUTION/AVAILABILITY STATEMENT
Approved for public release, distribution unlimited

13. SUPPLEMENTARY NOTES

14. ABSTRACT

15. SUBJECT TERMS

16. SECURITY CLASSIFICATION OF:			17. LIMITATION OF ABSTRACT	18. NUMBER OF PAGES	19a. NAME OF RESPONSIBLE PERSON
a. REPORT	b. ABSTRACT	c. THIS PAGE			
unclassified	**unclassified**	**unclassified**	**UU**	**16**	

to enhance the repopulation and regeneration of the damaged tissue.[28] There is also a desire to deliver viable stem cells that will enable them to utilize the microenvironmental cues to differentiate into specific cell phenotype. Three-dimensional extracellular matrix (ECM) present in interstitial tissues is the prototypic substrate for cell migration, morphogenesis, immune defense, and wound repair. These tissues contain significant amounts of collagen as the extracellular matrix component. Integration of stem cells within a collagenous matrix as a seeding medium has been shown to enhance loading of the cells into scaffold and, more importantly, increase their proliferation during 3D culture.[29] The embedded cells were also shown to be fine tuned to differentiate into specific cell types in an optimized induction medium.[30–32]

Other scaffolds currently being used to regenerate viable tissues contain materials that vary widely in their chemical, mechanical, and structural properties. Natural polymers such as collagen, chitosan, alginate, and gelatin have been used extensively due to their biocompatibility and high efficiency to integrate with host tissue.[33] Stem cell therapy using polymeric micro- and nanocarriers based on these natural polymers (e.g., collagen, alginate, and fibrin) or synthetic polymers (e.g., poly lactide co-glycolic acid (PLGA) and poly-L-lysine) have been successfully used cell delivery devices.[34–38] Although these biomaterials have been shown to be conducive for cell growth and differentiation, when the cells are encapsulated inside the polymer matrix and congealed into spheres, the cells ability to proliferate and migrate into the damaged tissue is inhibited.[37]

To overcome the problem of the inability of encapsulated cells to migrate and still deliver them effectively, in this study we have loaded ASC within chitosan microspheres (CSM) carriers using cell culture insert technique. Chitosan was chosen since it is a cationic polysaccharide with excellent biocompatibility, porous structure, and gel-forming properties, it can be easily chemically modified, and it has a high affinity for *in vivo* macromolecules.[39,40] Therefore, chitosan acts to mimic the polysaccharide and glycosaminoglycan portion of the extracellular matrix, enabling it to function as a substrate for cell adhesion, migration, and proliferation. Recently, it has been shown that chitosan can be combined with other polymers, such as collagen and silk fibroin, and used as a delivery vehicle for adipose-derived stem cells and enhance soft tissue repair.[41,42] The ASC-loaded CSM–polymer composites were then evaluated *in vitro* as a cell delivery device and were shown to maintain viability within the microspheres and their multilineage differentiation potential after migrating from the microspheres.[41] In addition, the ASC-loaded microspheres were incorporated into collagen gel matrix and assessed for release from microsphere and phenotypic changes in the gel matrix.[41]

Materials and Methods

Isolation of adipose-derived stem cells

Rat ASC were isolated from perirenal and epididymal adipose tissue as previously described.[43] Perirenal and epididymal fat was collected and washed with sterile Hank's buffered balance solution containing 1% bovine serum albumin. The tissue was minced, transferred into 25 mL of Hank's buffered balance solution/1% bovine serum albumin, and centrifuged at 500 *g* for 5 min at room temperature. The free-floating adipose tissue layer was collected and treated with collagenase type II (200 U/mL; Sigma–Aldrich, St. Louis, MO) for 45 min at 37°C in an orbital shaker. The digested tissue was then filtered through 100 μm and 70 μm nylon mesh filter, centrifuged at 500 *g* for 10 min at room temperature, and washed twice with sterile phosphate-buffered saline (PBS). The cell pellet was resuspended in growth medium (MesenPRO RS™ Basal Medium) supplemented with MesenPRO RS Growth Supplement, antibiotic–antimycotic (100 U/mL of penicillin G, 100 μg/mL streptomycin sulfate, and 0.25 μg/mL Amphotericin B), and 2 mM L-glutamine (Gibco/Invitrogen, Carlsbad, CA). Cells were cultured on T75 flasks (BD Biosciences, San Jose, CA) and maintained in a 5% CO_2 humidified incubator at 37°C. Passage 2–4 ASC were used for all experiments.

Preparation of CSM

CSM were prepared by water-in-oil emulsification process along with an ionic coacervation technique using our previous protocol at room temperature.[45] Briefly, an aqueous solution of chitosan (6 mL of 3%w/v chitosan in 0.5 M acetic acid) was emulsified in an oil phase mixture consisting of soya oil and n-octanol (1:2 v/v) in the presence of 5% sorbitan-monooleate (span 80) emulsifier, using an overhead (1700 rpm) and magnetic stirring (1000 rpm) simultaneously. The mixture was continuously stirred for approximately 1 h until a stable water-in-oil emulsion was obtained, followed by the addition of 1% w/v of potassium hydroxide (1.5 mL/15 min for 4 h) in n-octanol to initiate ionic gelation. After completion of the crosslinking reaction, the oil phase of the mixture containing CSM was slowly decanted and the spheres were immediately added to 100 mL of acetone. The spheres were repeatedly washed with acetone until discrete, oil-free spheres were obtained. The recovered spheres were dried in a vacuum desiccator and sized using particle size analyzer (Malvern Mastersizer E–Laser, Malvern, United Kingdom). For subsequent experiments CSM were sterilized using absolute alcohol and washed three times with sterile water to remove residual salts.

Free amino groups in CSM

The number of free amino groups present in CSM, before and after ionic gelation, was determined using the trinitro benzenesulfonic (TNBS) acid assay of Bubins and Ofner.[46] Briefly, a known amount of microspheres (5–10 mg) was incubated with 1 mL of 0.5% TNBS solution for 4 h at 40°C and hydrolyzed using 3 mL of 6N HCl at 60°C for 2 h. Samples were cooled to room temperature, and 5 mL of deionized water was added and extracted with 10 mL of ethyl ether. A 5 mL aliquot of the aqueous phase was warmed to 40°C for 15 min to evaporate any residual ether, cooled to room temperature, and then diluted with 15 mL of water. The absorbance was measured at 345 nm using a Beckman Coulter DU 800 UV/Visible Spectrophotometer (Beckman, Brea, CA) against TNBS solution without chitosan as blank, and the chitosan used for sphere formation was used as a standard for total amino group. The relation between absorbance and percentage of free amino groups relative to chitosan was estimated.

Loading ASC in CSM

Sterilized CSM (5 mg) equilibrated in sterile PBS overnight were added to culture plate inserts with an 8 μm pore size membrane (24-well format; BD Biosciences, San Jose, CA),

after the CSM settled, the PBS was aspirated and replaced with 300 μL of growth medium. ASC resuspended in 200 μL of medium were seeded at different concentrations (1×10^4 to 4×10^4) over the CSM in culture inserts. The final volume of medium within the culture insert, after seeding, was 500 μL, and the volume of medium surrounding the insert was 700 μL. Cells seeded on CSM were incubated for 12, 24, 48, 72, and 96 h in a humidified incubator at 37°C and 5% CO_2.

Percentage ASC loading and cell viability in CSM

After incubation the ASC-loaded CSM were collected in sterile 1.5 mL microcentrifuge tubes without disturbing the cells that had migrated into the insert membrane. The residual medium was removed and 250 μL of fresh growth medium was added. To each tube 25 μL MTT [3-(4,5-dimethylthiozole-2-yl)-2,5-diphenyltetrazolium bromide; Sigma-Aldrich, St. Louis, MO] solution (5 mg/mL) was added and incubated for 4 h in a 5% CO_2 humidified incubator at 37°C.[47] After incubation the medium was removed, 250 μL of dimethyl sulfoxide (Sigma-Aldrich) was added, and the mixture was vortexed for 2–5 min to solubilize the formazan complex. CSM were then centrifuged at 2700 *g* for 5 min, and the absorbance of supernatant was measured at 570 nm with 630 nm as reference using Molecular Devices Spectramax M2 Microplate Reader (Molecular Devices, Sunnyvale, CA). Similarly, cells in the culture inserts were treated with MTT, the formazan complex solubilized with dimethyl sulfoxide was collected, and the absorbance of supernatant was measured. The cell number associated with the CSM and those on the insert was determined relative to the standard absorbance value obtained from known numbers of viable ASC.

Fluorescent and confocal microscopic morphological analysis of ASC in CSM

ASC were cultured with CSM for 24 h, incubated with 2 μM Calcein AM (Sigma-Aldrich) for 30 min, and washed twice with PBS. The cells were observed for viability using an Olympus IX71 inverted microscope equipped with a reflected fluorescence system (Olympus America, Center Valley, PA). Photomicrographs of Calcein acetoxymethyl ester (AM) stained and unstained cells were taken using a DP71 digital camera, and overlay of images was carried out using DP controller application software. To obtain 3D images, optical sections of Calcein AM stained cells were taken using an Olympus FV-500 Laser Scanning Confocal Microscope (Olympus America), equipped with a three-channel detection system for fluorescence, a differential interference contrast image laser light source, and a Z-stepper motor. The 3D stereoscopic images were generated from a series of Z-stacked photomicrographs using Fluoview and Tiempo Ratio Imaging software, and final images were processed using Image J software (image processing and analysis in Java; NIH, Bethesda, MD).

ASC–CSM-embedded collagen gel and characterization

Before culturing ASC in CSM, the cells were cytoplasmically labeled with quantum dot (Qdot) nanocrystals 565 using Qtracker cell labeling kit (Molecular Probes/Invitrogen, Carlsbad, CA). Cells were labeled according to the manufacturer's instructions. Briefly, 10 nM of labeling solution was incubated for 5 min at 37°C, and to this solution 200 μL of MesenPRO medium was added and vortexed; 1 mL of cell suspension (1×10^6 cells) was added to the labeling solution and incubated for 45 min at 37°C, 5% CO_2.

Qdot-labeled ASC were cultured in CSM (5 mg) for 24 h, collected, and mixed with type 1 collagen (7.5 mg/mL) extracted from rat tail tendon according the method of Bornstein[48] and fibrillated by adjusting the pH to 6.8 using 2N NaOH. The fibrillated collagen–ASC–CSM mixture was added to a 12-well plate and incubated for 30 min at 37°C. After complete gelation the collagen–ASC–CSM gels were incubated for 14 days at 37°C, 5% CO_2. Release of cells was observed, and light and fluorescent pictures were taken at different days using an Olympus IX71 inverted microscope equipped with reflected fluorescence system. Gels were cryopreserved as previously described.[44] Briefly, collagen–ASC–CSM gels were treated serially with increasing concentrations of sucrose (from 5% and 20%) and then incubated overnight with 20% sucrose. The sucrose-treated gels were flash frozen after embedding them in a 20% Sucrose–Histoprep™ (Fisher, Pittsburgh, PA) mixture (2:1). Sections of 10–12 μm were cut, fixed for 20 min with 4% paraformaldehyde, washed twice with Hank's balanced salt solution (5 min each), and viewed under an inverted fluorescence microscope. To assess the phenotype of cells that have migrated into collagen matrix, sections were stained with Stro-1 antibody and epifluorescence images were taken.

Scanning electron microscopy

ASC were cultured on CSM for 24 h and fixed (4% v/v formaldehyde, 1% v/v glutaraldehyde in PBS) for scanning electron microscopic analysis. The samples were rinsed in 0.1 M phosphate buffer (two times, 3 min each) and then placed in 1% Zetterquist's Osmium (Sigma–Aldrich) for 30 min. The samples were then dehydrated in ethanol (70% for 10 min, 95% for 10 min, and 100% for 20 min), treated with hexamethyldisilizane (two times, 5 min each) (Polysciences, Warrington, PA), and air-dried in a desiccator. The specimens were sputter-coated with gold–palladium (40%/60%) and observed with a Leo 435 VP scanning electron microscope (Carl Zeiss MicroImaging, Thornwood, NY) in high-vacuum mode at 15 kV.

Transmission electron microscopy

ASC cultured with CSM and ASC–CSM cultured in collagen gel (14 days postculture) were fixed in 1% v/v glutaraldehyde in PBS. The samples were rinsed in 0.1 M phosphate buffer (two times, 3 min each) and then placed in 1% Zetterquist's Osmium for 30 min. The samples were subsequently dehydrated in a series of ethanol washes (70% for 10 min, 95% for 10 min, and 100% for 20 min), treated with hexamethyldisilizane (two times, 5 min each), and finally air-dried in a desiccator. Samples were then washed and infiltrated with epoxy resin. Ultrathin sections (~70 nm) were cut, and sections were examined on a JOEL 1230 transmission electron microscope (Joel, Boston MA).

Migration, maintenance of stem cell phenotype, and differentiation of ASC in CSM

ASC were incubated with CSM for 24 h and carefully collected as described above. The ASC–CSM were then transferred to a new culture dish and incubated for 48 h.

Third-generation ASC from the CSM were analyzed for expression of stem-cell-specific markers and potential to differentiate into adipogenic- and osteogenic-type cells.

Immunophenotype of ASC that migrated out from CSM

Flow cytometry (fluorescence-activated cell sorting [FACS]) analysis and immunocytochemical staining of ASC that migrated out from the CSM were performed to characterize expression of stem-cell-specific surface markers.

Immunocytochemical staining. Third-generation ASC from the CSM were incubated on a 2-well chambered slide (Nalge Nunc; LabTek® chamber slide, Noperville, IL) for 48 h. The cells were washed twice with sterile PBS and fixed with 10% buffered formalin. Fc-receptor-mediated blocking sites were blocked by incubating the cells for 20 min with 1 μg (/10^4 cells) of BD Fc Block™ Block Solution (BD Bioscience, San Jose, CA) or nonpermeant blocking solution containing 5% donkey serum (Sigma-Aldrich) in Dulbecco's PBS. Cell surface markers were identified by incubating ASC overnight at 4°C with 10 μg of fluorescein isothiocyanate (FITC)–conjugated anti-mouse monoclonal antibodies against CD45 (leukocyte common antigen), CD49d (integrin α-4, CD54 (ICAM-1), CD71 (transferrin receptor), CD90 (Thy-1 glycoprotein), CD106 (VCAM-1), and Sca-1 (stem cell antigen-1, Ly-6A/E) (BD Bioscience), and CD105 (Endoglin) (R&D Systems, Minneapolis, MN). To observe Stro-1 (R&D Systems) expression, cells were fixed with 10% buffered formalin for 15 min, washed twice with PBS, blocked with 2% serum, and incubated overnight at 4°C with 10 μg of Stro-1 and FITC-labeled anti-mouse IgG secondary reagent (R&D Systems). Nonspecific fluorescence was determined using equal aliquots of cell preparation incubated with an FITC-labeled anti-mouse IgG secondary reagent. All surface antigens were also tested with ASC before culturing them with CSM as controls.

Flow cytometry (FACS). Control ASC (passage 3) and third-generation ASC from the CSM were cultured for 48 h. Cells were washed twice with Hank's balanced salt solution, trypsinized, and suspended in FACS cell staining buffer (Biolegend, San Diego, CA) to a final concentration of 5×10^5 cells/100 μL. Cells were directly labeled for cell surface markers by incubating them for 45 min with primary antibodies against CD54-FITC, CD71-Phycoerythrin (PE), and CD90-PE. Cells were stained for Stro-1 indirectly by incubating them with monoclonal antibody against Stro-1 for 45 min after which they were washed with cell staining buffer twice (5 min each) and stained with FITC-labeled anti-mouse IgM as a secondary reagent for 1 h. Cells were washed twice and then resuspended in 500 μL of cell staining buffer. FACScan was performed using a FACSAria flow cytometer (Becton–Dickinson, Mt. View, CA). Results were quantitated by FACSDiva software (BD Biosciences, Mt. View, CA). Twenty thousand cells were analyzed, and the total population positive for specific cell surface markers is tabulated. Cells stained with FITC and PE-conjugated nonspecific IgG were used to determine background fluorescence.

Adipogenic differentiation of ASC migrated from CSM

Third-generation ASC were cultured to confluence and induced with adipogenic differentiation medium composed of Dulbecco's modified Eagle's medium (Gibco/Invitrogen) supplemented with 10% fetal bovine serum, dexamethasone (1 μM), indomethacin (200 μM), insulin (10 μM), isobutylmethylxanthine (0.5 μM) (Sigma-Aldrich), 2 mM L-glutamine, and antibiotic–antimycotic, and were cultured in a 5% CO_2 humidified incubator at 37°C for 21 days.[43] To observe the staining of neutral lipids, cultures were rinsed with PBS, fixed with 10% buffered formalin solution, and stained with Oil Red O (Sigma-Aldrich). ASC, before culturing with CSM, but treated under similar conditions were used as controls. For adipogenic differentiation of ASC that migrated into the collagen gel from CSM, ASC (40,000)-loaded CSM were embedded in collagen matrix and induced to differentiate with adipogenic medium and observed for 24 days. They were fixed with 4% paraformaldehyde and stained with Oil Red O (Sigma-Aldrich) to observe the staining of differentiated cells in collagen gel. Undifferentiated ASC–CSM in collagen matrix served as controls.

Osteogenic differentiation of ASC migrated from CSM

Third-generation ASC were cultured to confluence and induced with osteogenic differentiation medium composed of α-minimal essential medium (α-MEM) (Gibco/Invitrogen) supplemented with 10% fetal bovine serum, dexamethasone (0.1 μM), Ascorbate-2-phosphate (50 μM), β-glycerophosphate (10 mM), bone morphogenic protein-2 (BMP-2, 10 ng/mL; R&D Systems), 2 mM L-Glutamine (Sigma-Aldrich), and antibiotic–antimycotic, and cultured in a 5% CO_2 humidified incubator at 37°C for 26 days. Cultures were rinsed with PBS and fixed with 10% buffered formalin solution and calcium phosphate deposition by staining with Alizarin red S (Sigma-Aldrich). ASC, before culturing with CSM, treated under similar conditions were used as controls.[43]

RNA isolation and real-time polymerase chain reaction

Total RNA from passage 3 ASC (control) and third-generation stem cells migrated out from the CSM before and after adipogenic and osteogenic differentiation were isolated using Trizol reagent (Invitrogen, Carlsbad, CA).[49] The concentration of RNA was determined at $OD_{260/280}$ using a NanoDrop spectrometer (NanoDrop Technologies, Wilmington, DE). Complementary DNA was synthesized from 150 ng of total RNA, in duplicates, using SuperScript™ III first-strand synthesis supermix with oligo-dT primers (Invitrogen). A control lacking the RNA sample was synthesized for each primer, to detect the random production of cDNA through contaminants. Oligonucleotide primer sequences specific to stem cell surface markers (CD49d, CD54, CD71, CD90, and Sca-1) and adipogenic (Glucose transporter-4 [Glut-4], Adiponectin, Peroxisome proliferator-activated receptor γ [PPAR-γ], leptin, Fatty acid binding protein-4 [Fabp-4]) and osteogenic (alkaline phosphatase [ALP], osteonectin, osteopontin, osteocalcin, and bone morphogenic protein-2 [BMP-2]) differentiation-specific genes were purchased from SA Biosciences (Frederick, MD). Master mixes containing 200 nM of forward and reverse primers with SYBR® Green-ER™, qPCR supermix (Invitrogen), and the synthesized cDNA were added to appropriate wells. Real-time polymerase chain reaction (RT-PCR) was carried out using a Bio-Rad CFX96 thermal cycler system (Bio-Rad, Hercules, CA). mRNA expression levels were normalized to glyceraldehye-3-

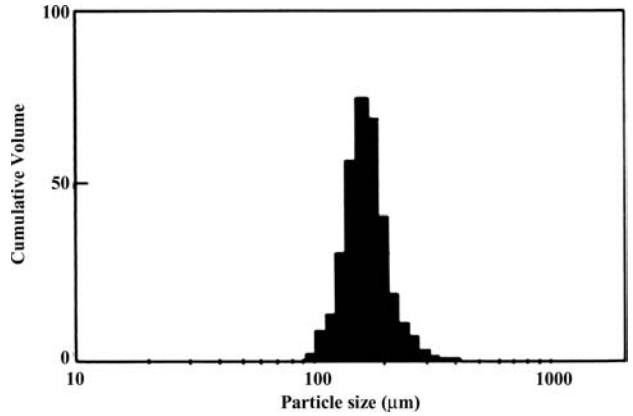

FIG. 1. Chitosan microsphere (CSM) size distribution. The microsphere size distribution pattern indicates that more than 90% of spheres are between 175 and 250 μm in diameter.

phosphate dehydrogenase mRNA levels. Fold increase in expression levels for each stem-cell-specific, adipogenic, and osteogenic gene was normalized to the expression levels of control passage 3 ASC.[50]

Results

CSM and cell loading

CSM preparation involved the crosslinking of the heteropolysaccharide chains of chitosan through simple ionic interactions of $-COO^-$ ions with K^+ ions. The spheres are formed using water-in-oil emulsion technique and potassium hydroxide, in oil phase, as the polysaccharide chain crosslinker. This method yielded evenly sized spheres of 175–250 μm range (>90%) with uniform crosslinking of the matrix from core to the surface (Fig. 1). The microspheres form a porous network and upon hydration have a swelling capacity ≈1.6-fold their original size while maintaining a spherical morphology. Upon analysis of several preparations of microspheres, it was determined that they have only a slight variation in the percentage of free $-NH_2$ group (98.8 ± 2) with respect to chitosan, indicating that the amino groups are unaffected after processing.

Previous experiments using various concentrations of microspheres indicated that 5 mg of CSM was an optimal amount to form a single layer on a 24-well cell culture inserts and was used for the following experiments. Using ASC, passage 3, seeded over evenly layered CSM on a culture insert with a membrane pore size of 8 μm shows that the cells actively migrated both onto and into the spheres and were viable when assessed after 96 h. The number of viable cells increased proportionally from the initial seeding concentration (Fig. 2A), and a maximum number of cells were found to migrate into the CSM after 24 h. There was a slight decrease in cell number after 24 h (≈10–12% with respect to initial cell loading of 30,000 and 40,000, respectively), after which the cell density on the collected microspheres remained relatively constant through 96 h.

The number of cells left on the cell culture inserts after ASC loading onto the CSM showed a constant increase in cell number (Fig. 2B). In the culture inserts in which the CSM had been initially seeded with 10,000 and 20,000 cells, the cell number increased through 96 h, whereas in culture inserts in which the CSM had been initially seeded with 30,000 and 40,000 cells, the number of cells on the culture inserts

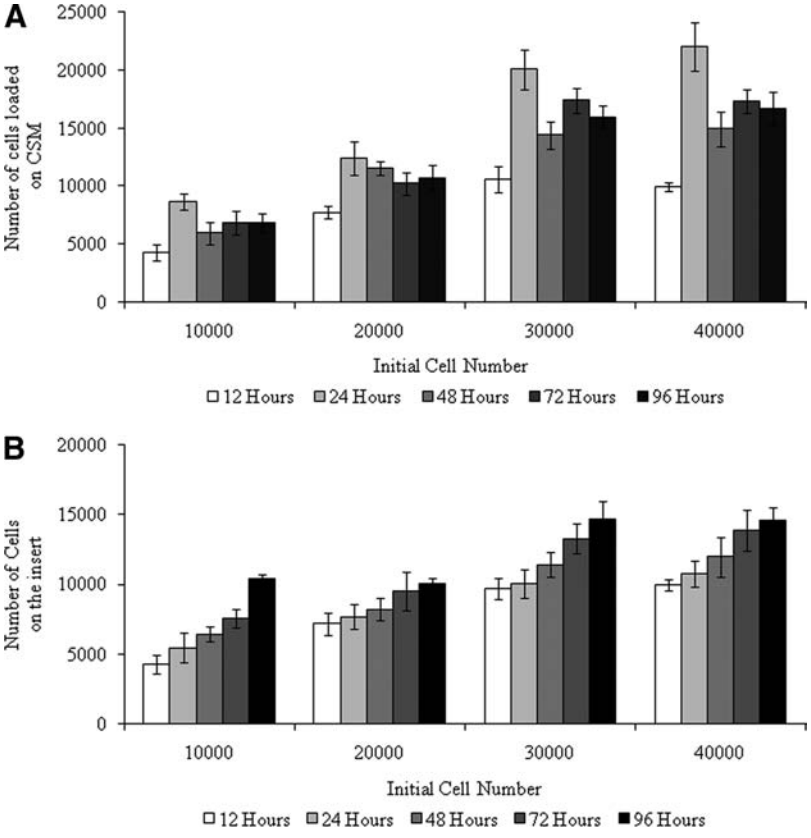

FIG. 2. Adipose-derived mesenchymal stem cell (ASC)–CSM cell viability time course. (**A**) Bar graph representing the percentage of ASC attached to the CSM with respect to time (mean% ± SD, $n = 3$). (**B**) Bar graph representing the number of cells remaining on the culture well insert after CSM loading (mean ± SD, $n = 3$).

proliferated up to 72 h and did not significantly increase after that time point. The increase in cell number can be attributed to cell proliferation on the insert over time, which occurs until the cells reach confluence. These results indicate that efficient cell loading was achieved with an initial cell seeding density of 3×10^4 cells/5 mg CSM, which resulted in adhesion and migration of $\approx2\times10^4$ cells/5 mg of CSM (67%) by 24 h (Fig. 2A), and these conditions were used for all other experiments.

Morphological characterization of ASC in CSM

To determine the viability and location of the adipose-derived stem cells that had attached to the microspheres, ASC were cocultured with CSM and analyzed using the fluorescent cytoplasmic probe Calcein AM. Figure 3A shows a light micrograph of the ASC migrating and attaching to the CSM polymeric matrix. Fluorescence of metabolically active cells shows an equal distribution of ASC over the complete CSM microsphere (Fig. 3B). Higher magnification epifluorescence of the cells shows that they are attached on the surface (Fig. 3C), as well as having migrated into the spheres, as shown when focused beyond the boundaries of CSM (Fig. 3C inset). These results were further confirmed using confocal imaging (Fig. 3D–F). ASC on the surface exhibited elongated fibroblast-like morphology (Fig. 3E), whereas cells that had migrated inside the microsphere had retracted filopodia with a smaller overall cytoskeletal structure. Figure 3F, an overlay of a Z-stacked fluorescent image and the differential interference contrast image, demonstrates cytosolic Calcein AM of ASC to be spread over on the surface and smaller, more discrete staining of ASC from cells that have migrated inside the microspheres.

The ultrastructural imaging by scanning electron microscopy shows the porous microspheres and adipose stem cells that are tightly adhered to the surface of the spheres (Fig. 4A). The cells have a flat, elongated morphology, capable of stretching across large areas on the surface of the microspheres (Fig. 4B). At higher magnification it is apparent that the cells were also to interact with the chitosan matrix by extending filopodia on the porous structures of the spheres (Fig. 4C, arrows), similar to what was observed with the confocal microscope (Fig. 3).

Further analysis by transmission electron microscopy showed the ultrastructural morphology of ASC in CSM. A serial cross section of an ASC–CSM (Fig. 5A) revealed the porous nature of the microsphere that enables the ASC to attach and migrate into the microspheres (Fig. 5B). The ASC retained their overall morphology and intracellular components (Fig. 5C), while readily attaching to the surface and migrating into the pores of the CSM by extending their filopodia (Fig. 5D, E). Examination at high magnification shows the infiltration of intact cellular components into the porous structures of the CSM (Fig. 5F), confirming the ability of ASC to utilize the CSM 3D architecture for attachment.

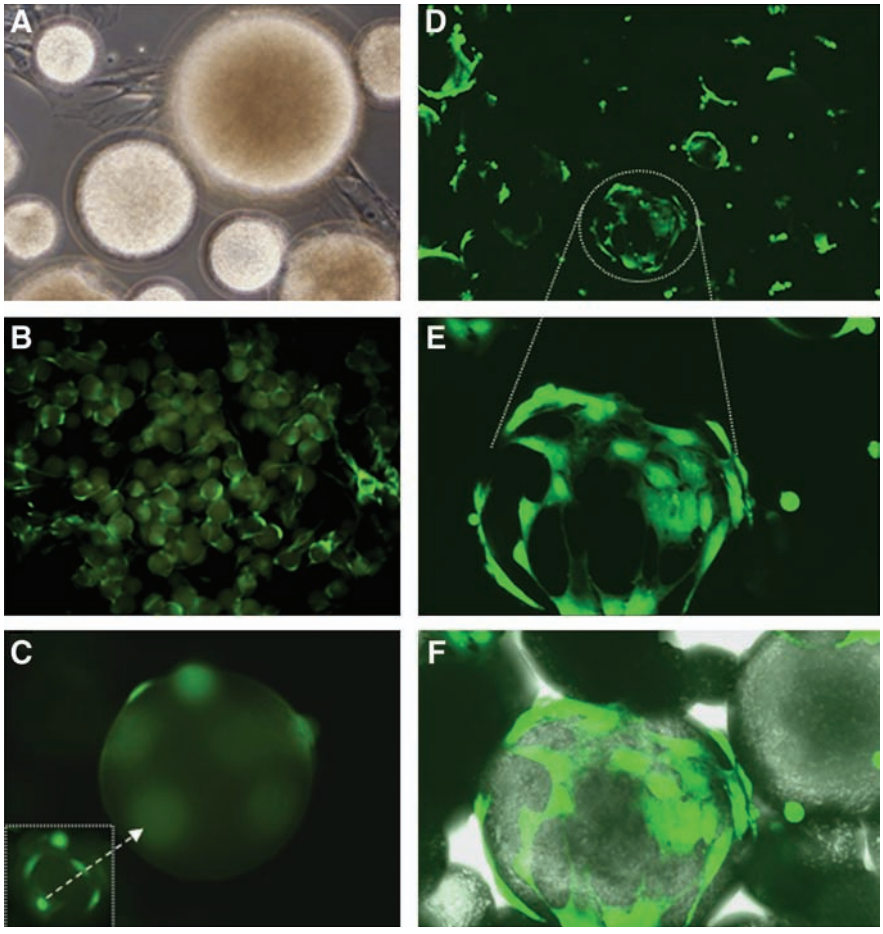

FIG. 3. Morphological features of Calcein AM–stained ASC–CSM. (**A**) Phase contrast image (magnification, ×20) after 24 h showing attachment of ASC to CSM. (**B**) Epifluorescence image (magnification, ×10) showing distribution of ASC on CSM. (**C**) Epifluorescence image (magnification, ×20) of ASC on a single microsphere; inset image is focused beyond the boundaries of the CSM to observe morphology of ASC that have migrated into the core of the CSM. (**D, E**) Confocal images (magnification, ×20, 20×3.5, respectively) showing three-dimensional distribution of ASC. (**F**) Confocal Z-stacked image with differential interference contrast overlay of the ASC geometric location within the CSM. Color images available online at www.liebertonline.com/ten.

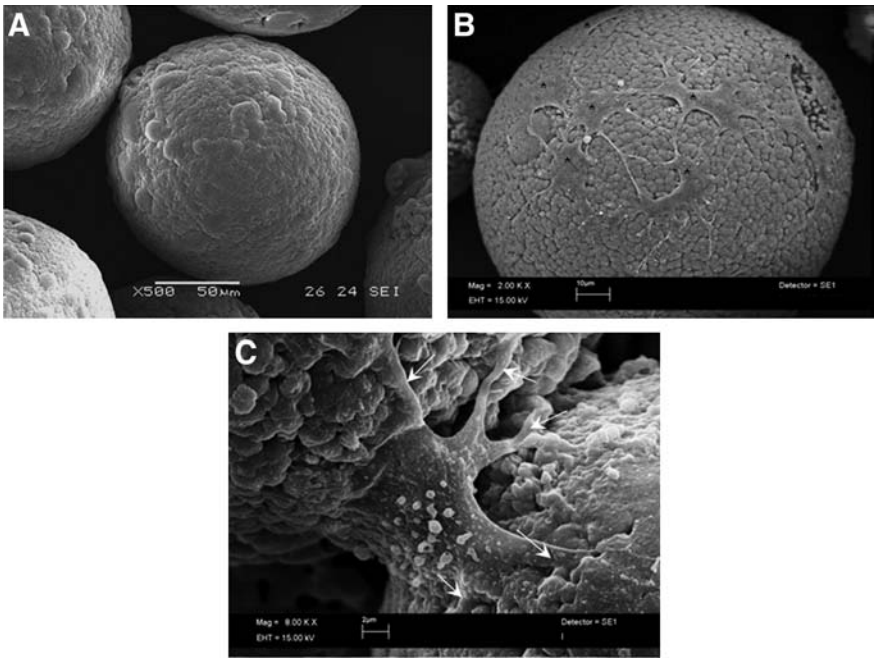

FIG. 4. Scanning electron microscopic images of ASC and CSM. (**A**) CSM alone, indicating the porous and spherical morphology of CSM. (**B**) Co-cultured ASC and CSM with cells (marked by asterisks) strongly adhered to CSM with flat and elongated morphology. (**C**) Attachment of ASC into CSM using filopodia (indicated by arrows).

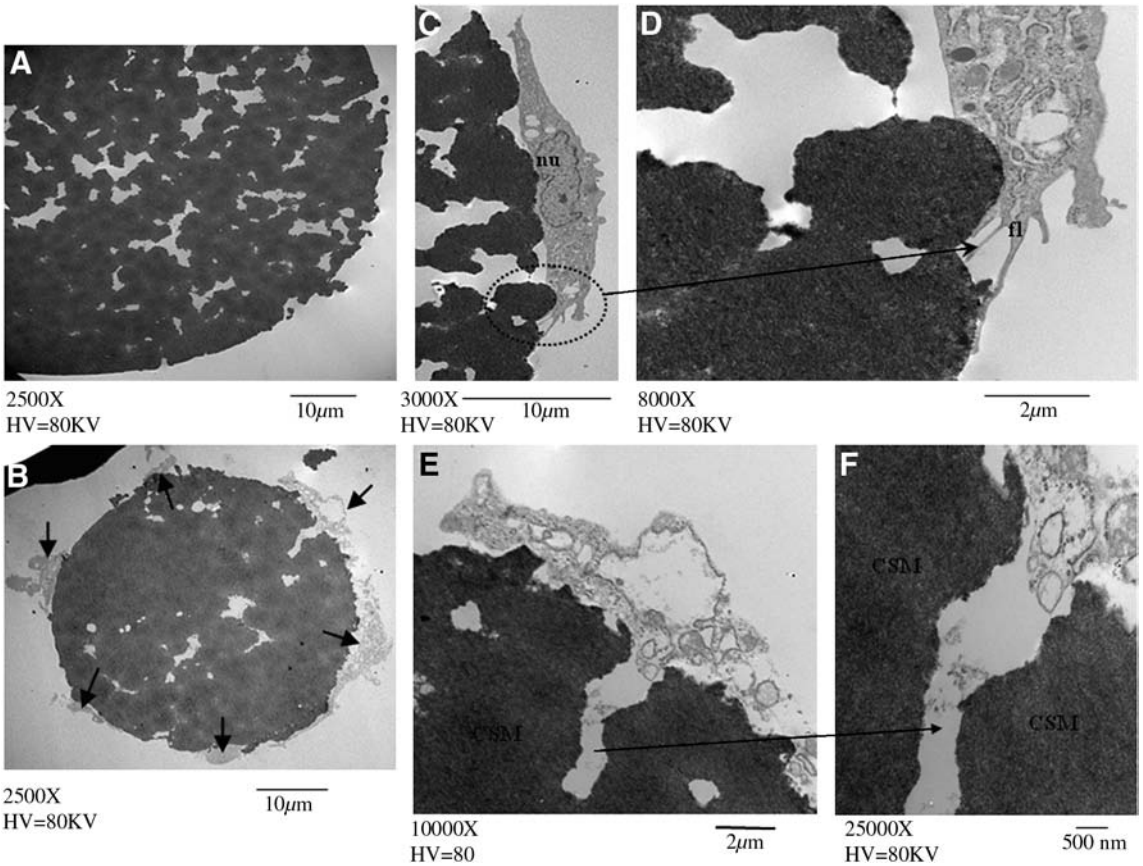

FIG. 5. Transmission electron microscopic (TEM) images of ASC and CSM. (**A**) Ultra-thin cross section of porous CSM. (**B**) Cocultured ASC and CSM showing the gross distribution and ultrastructure of ASC on CSM (indicated by arrows). (**C**) High magnification of ASC attached to CSM with intact cellular components (nu, nucleus). (**D**) ASC–CSM showing attachment of filopodia (fl) extended into CSM. (**E**) ASC invading into CSM through the pores. (**F**) High magnification showing infiltration/invasion of ASC into the CSM and extension of cellular components.

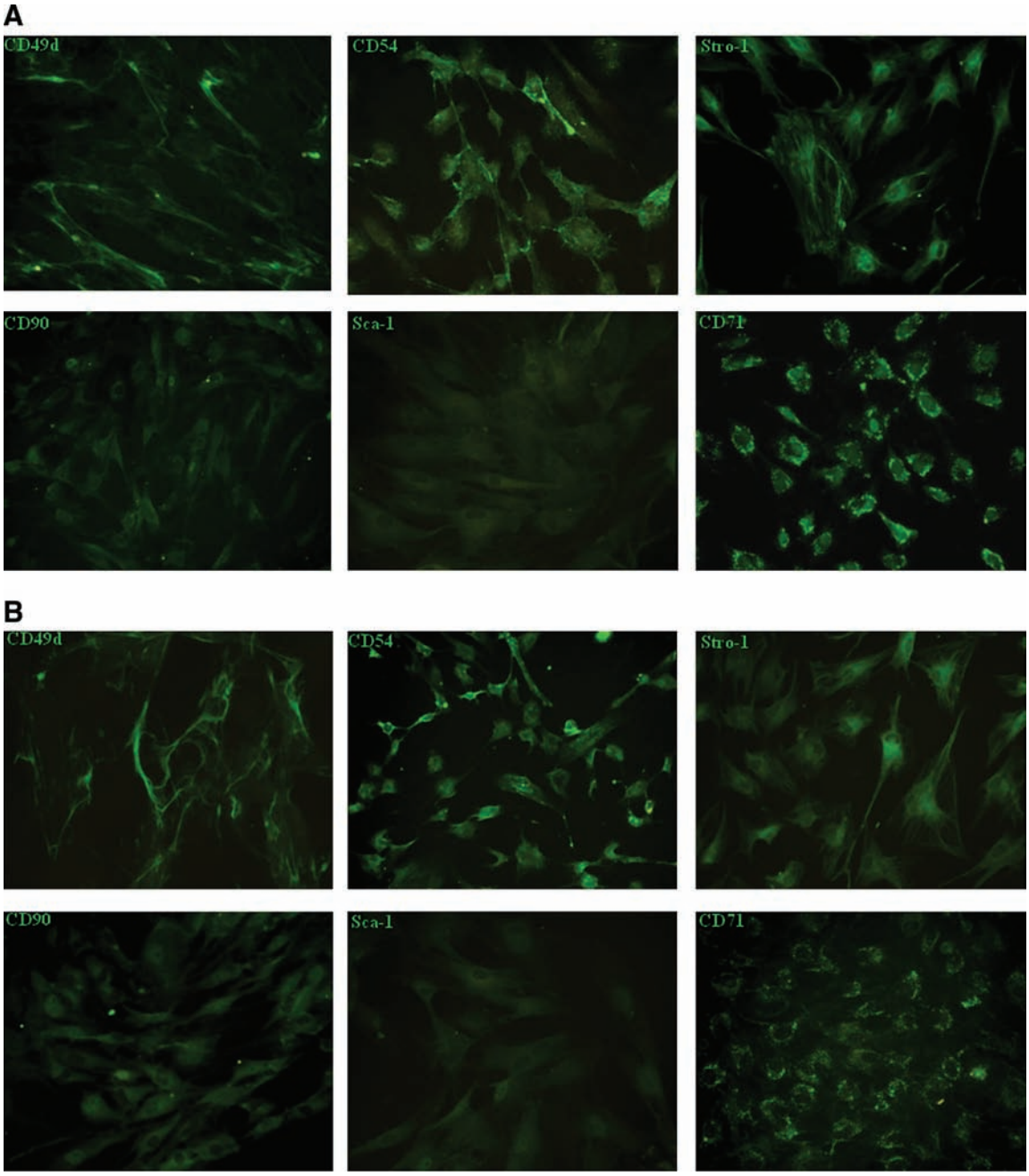

FIG. 6. Immunofluorescent images of stem cell surface markers. (**A**) Photomicrographs of markers expressed in control ASC and (**B**) ASC that migrated out from CSM. Figures in each panel indicate the specific cell surface marker. All antibodies, except Stro-1, are fluorescein isothiocyanate (FITC)–labeled primary antibodies. Stro-1 is identified using isotype-matched FITC-labeled rat IgM. All photomicrographs at 20× magnification. Color images available online at www.liebertonline.com/ten.

Migration and maintenance of stem cell phenotype of ASC in CSM

To determine the ability of the ASC to migrate out of the CSM, ASC-loaded CSM (5 mg) were transferred and re-plated. Immediately after plating, the cells start to migrate from the spheres, initially forming small colonies around CSM, changing to a slender fibroblast-like morphology, and are completely adhered to the dish by 12 h (data not shown). The migrated cells were able to proliferate and reached a confluent monolayer within 72 h of plating.

Using immunofluorescence the migrated ASC from the CSM were further characterized for expression of stem-cell-specific surface markers to ensure their ability to preserve the stem cell phenotype after migration. Third-passage control ASC (Fig. 6A) were compared to ASC that had migrated from the CSM (Fig. 6B). The migrated ASC showed positive expression of CD49d (integrin α4) and CD54 (ICAM-1), considered key for cell–cell and cell–matrix interactions (Fig. 6B). Consistent with recent observations to specific stem cell surface proteins, the migrated ASC were also Stro-1 positive.[51] Further, they expressed positive stromal-associated markers

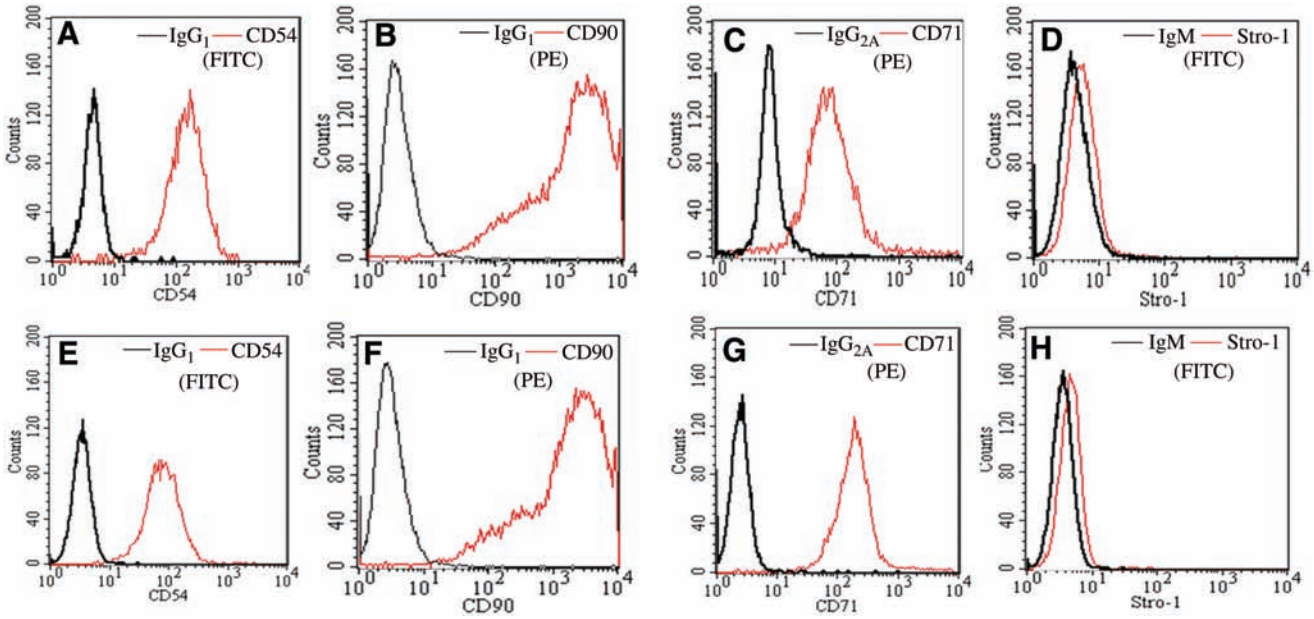

FIG. 7. Fluorescence-activated cell sorting analysis of control ASC (**A–D**) and ASC that migrated out from CSM (**E–H**). Stem-cell-specific markers (CD54, CD71, CD90, and Stro-1) were examined by flow cytometry. Cells were stained with FITC-labeled CD54 and phycoerythrin (PE)-labeled CD 71 and CD90 primary antibodies. Stro-1 was indirectly stained with FITC-labeled monoclonal IgM after staining with rat-specific monoclonal Stro-1 antibody. Fluorochrome-conjugated nonspecific IgG_1, IgG_{2A}, and IgM were used as isotype controls for CD54 and CD90, CD71, and Stro-1, respectively. Color images available online at www.liebertonline.com/ten.

CD90 (Thy-1 surface glycoprotein) and Sca-1 (stem cell antigen) and CD71 (transferrin receptor antigen) (Fig. 6B).

Flow cytometry analysis (FACS) confirmed that when compared to control ASC (Fig. 7A–D) the migrated ASC from the CSM had retained stem-cell-specific surface markers (Fig. 7E–H). The FACS scan analysis shows that for the migrated ASC more than 95% of the total cell population analyzed were positive for CD54, CD71, and CD90. Consistent with previous reports,[51] for both control ASC and ASC that had migrated from CSM, the percentage of Stro-1-positive cells was significant, but low when compared to the other markers used (Fig. 7D, H; Table 1).

The investigation of the expression levels of stem-cell-specific genes (CD49d, CD54, CD71, CD90, and Sca1) shows that the ASC migrated from CSM show relative expression levels of mRNA to control ASC (Fig. 8). The expression levels of CD49d, CD54, and CD90 were one- to twofold higher than the control ASC, whereas CD71 and Sca1 expression in the cells out of microspheres was 0.5–1.0-fold lower. Therefore, the stem-cell-specific gene expression in control ASC versus ASC that had migrated out of microspheres did not change significantly.

Table 1. Fluorescence-Activated Cell Sorting Analysis of Percentage of Total Cells Positive for Stem-Cell-Specific Markers

	Positive events (% total)	
Markers	*ASC*	*ASC migrated out of CSM*
CD54	95.86	95.14
Stro-1	1.2	1.41
CD71	75.28	96.05
CD90	96.33	95.17

ASC, adipose-derived mesenchymal stem cells; CSM, chitosan microspheres.

Migrated ASC exhibits adipogenic and osteogenic differentiation

To determine whether the ASC maintained their pluripotency after migrating from the microspheres, the cells were differentiated to adipogenic or osteogenic lineages using standard induction conditions and compared to passage 3 control ASC. The cells were grown to confluence and the medium was switched to adipogenic or osteogenic

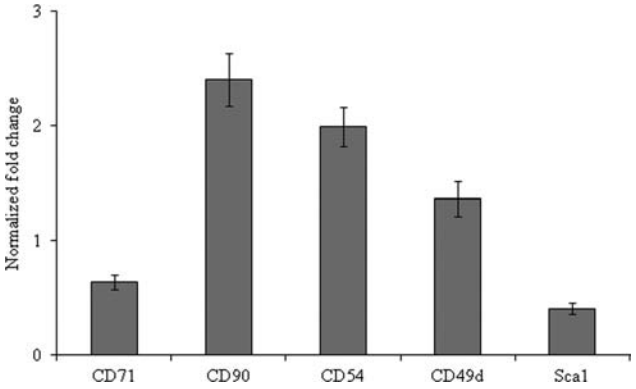

FIG. 8. Real-time polymerase chain reaction analysis of stem-cell-specific markers of ASC migrated out from CSM. Bar graph represents the normalized fold-induction relative to control ASC of mRNA levels of stem-cell-specific genes, CD90, CD54, CD49d, CD71, and Sca1. Values are mean fold change ± standard error of the mean.

medium to induce the ASC to differentiate into adipocytes or osteoblasts, respectively. The ASC differentiated into adipocytes had exhibited intracellular deposition of lipid droplets, which increased over time as observed by positive Oil Red O staining (Fig. 9A, B). When induced with osteogenic medium, the cells showed mineralized deposits increasing over time, as confirmed by Alizarin Red S staining for calcium deposition present in the differentiated the cells (Fig. 9C, D).

To determine the differentiation ability of ASC that had migrated out of CSM, adipogenic- and osteogenic-specific

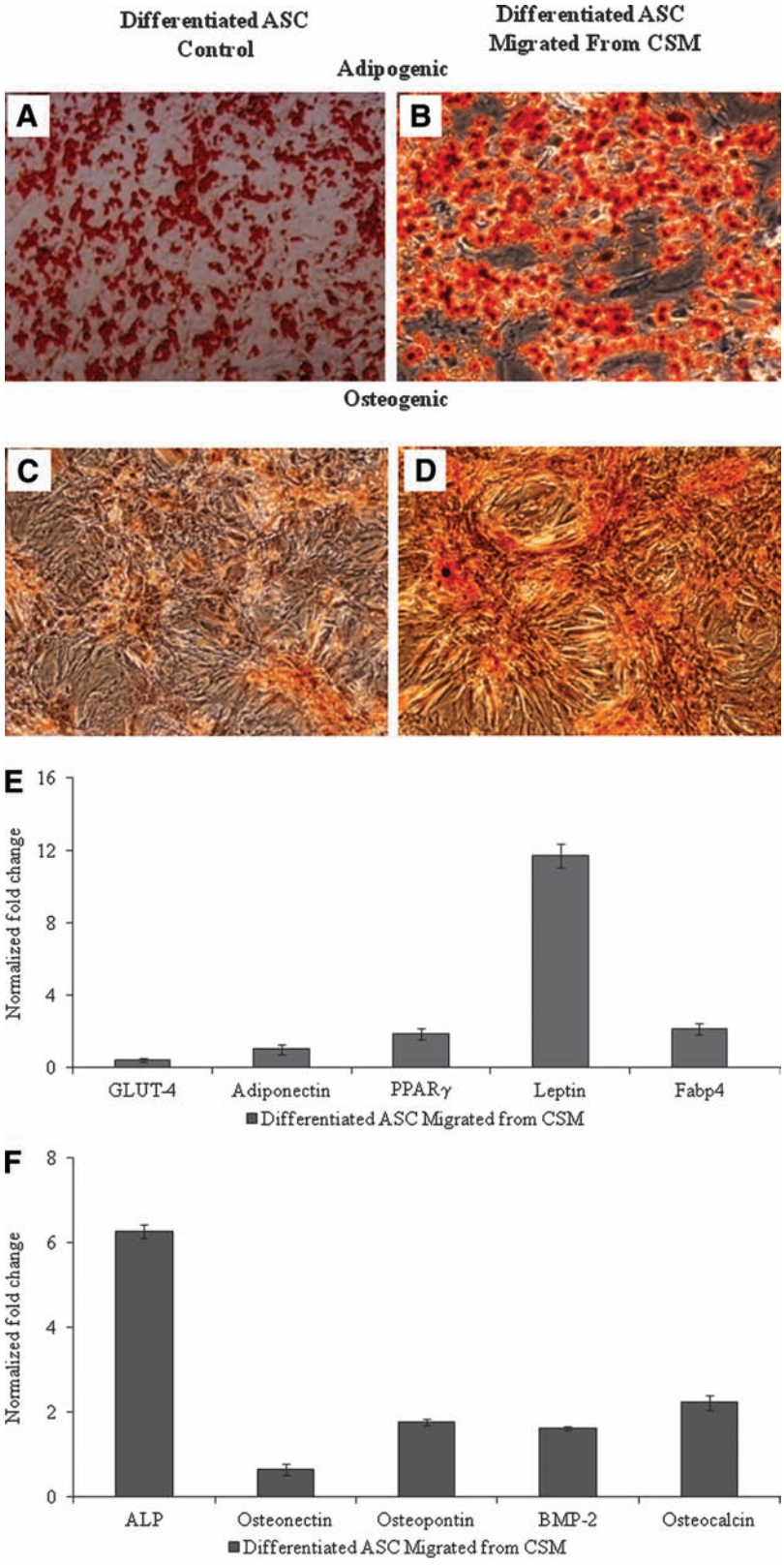

FIG. 9. Phase contrast photomicrographs showing ASC differentiation. Control ASC (**A, C**) and ASC that migrated out of CSM (**B, D**) induced to differentiate with adipogenic and osteogenic medium and stained with Oil Red O (**A, B**) and Alizarin Red S (**C, D**), respectively. All photomicrographs at 20× magnification. Real-time polymerase chain reaction analysis (**E, F**) of adipogenic- and osteogenic-specific genes for ASC migrated out from CSM normalized to control of ASC levels. Values are mean fold change ± standard error of the mean. Color images available online at www.liebertonline.com/ten.

gene expression was analyzed through RT-PCR. Figure 9E (adipogenic) and 9F (osteogenic) shows the normalized fold change in gene expression levels relative to differentiated passage 3 ASC. The ASC that had migrated from CSM showed an upregulation of adipose-specific genes above the control ASC levels. Leptin specifically had a dramatic increase in expression over the differentiated control cells (11.7-fold), whereas the other genes (Glut 4, adiponectin, and PPARγ) responsible did not change significantly relative to adipogenic differentiated passage 3 ASC. To confirm that the migrated ASC were pluripotent, the cells were differentiated to the osteogenic phenotype. Cells were examined for expression of ALP, osteocalcin, osteonectin, osteopontin, and BMP-2. There was a significant increase in ALP activity (6.2-fold), whereas expression levels of other genes (osteopontin, osteonectin, osteocalcin, and BMP-2) did not change significantly relative to osteogenic differentiated passage 3 ASC.

ASC migration from CSM into a collagen gel matrix

ASC labeled with Qdot 565 nanocrystals were used to monitor cell migration from the CSM into the collagen gels. Qdot-labeled ASC were loaded onto CSM, mixed into the collagen-based gel, and cultured for 14 days. Within 24 h, the ASC started migrating from the CSM into the surrounding gel matrix (Fig. 10A, B). The cells continued to migrate from the CSM into the collagen gel as shown at day 7 (Fig. 10C, D) and populated throughout the entire collagen gel by day 14 (Fig. 10E, F). This can be more clearly seen in frozen sections (Fig. 10G–J) of Qdot 565–labeled ASC–CSM in the collagen gel after 14 days of culture. Figure 10G is a bright field image showing the collagen fibrils and a CSM. Using fluorescence the Qdot-labeled ASC are observed migrating away from microspheres (Figure 10H, white arrows) into the collagen matrix. Figure 10I is an overlay of Figure 10G (converted to gray scale to show contrasting overlay) and 10H, which shows that at day 14 there are still Qdot-labeled ASC within the microspheres (asterisks) and cells that have migrated into the collagen matrix (arrows). Most importantly, the ASC that have migrated from the CSM retain their stem cell phenotype. This is clearly shown by the colocalization of Qdot-labeled ASC growing in collagen matrix stained with the stem-cell-specific marker Stro-1 (Figure 10J, white arrow).

TEM was used to analyze the morphology and ultrastructure of ASC that were released into the collagen gel from the CSM. Figure 11A is a representative image of cells releasing from the CSM and migrating into the collagen gel. The cells migrate away from the CSM by retracting their filopodia from

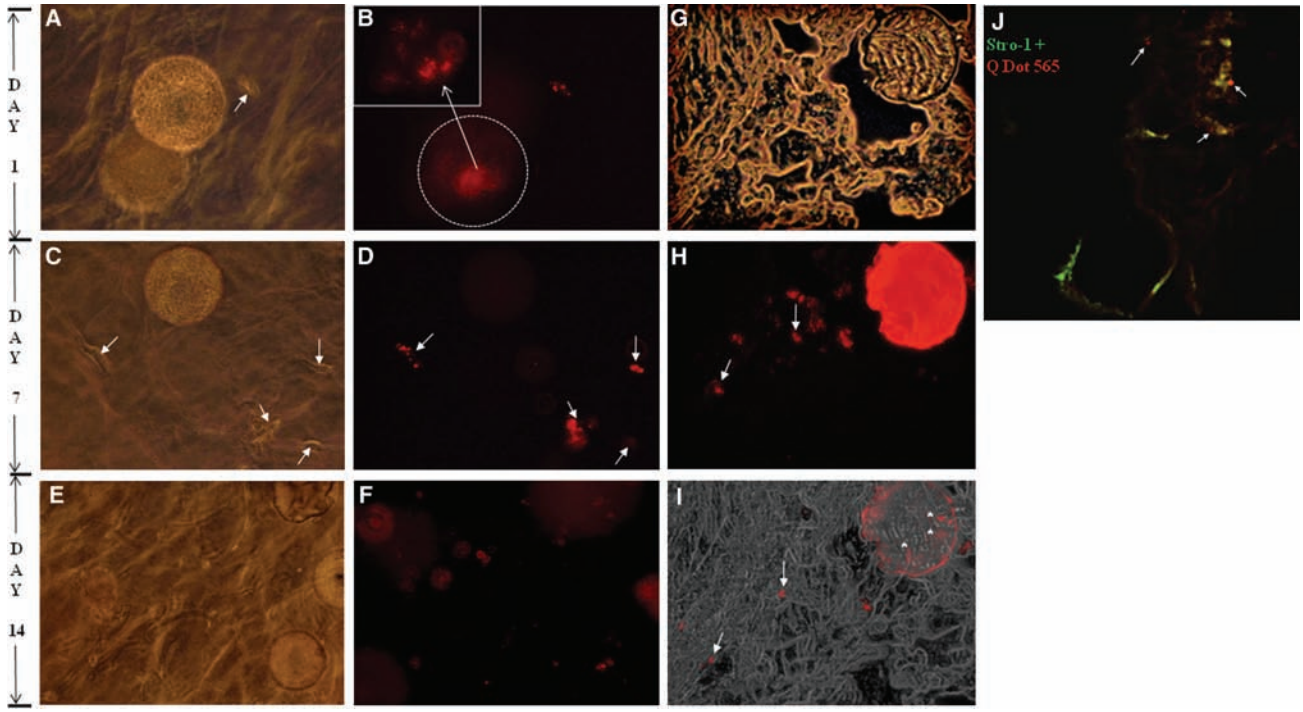

FIG. 10. Quantum dot labeled ASC–CSM in a collagen gel matrix. (**A**), (**C**), and (**E**) represent phase contrast images of ASC that have migrated from CSM and are attached on the collagen gel on days 1, 7, and 14, respectively. The white arrows (**A, C**) indicate the cells that have migrated from the spheres into collagen gel. (**B**), (**D**), and (**F**) represent fluorescent images of quantum dot (Qdot) 565–labeled ASC tracked after migration out from the CSM into the collagen gel on days 1, 7, and 14, respectively. (**D**) White arrows show Qdot labeled ASC. The inset in (**B**) is a magnified image of a microsphere showing ASC residing on the microsphere. The ASC slowly migrate from the CSM and populate the gel by day 14. All the images were taken at 20×magnification. Cryosections of quantum dot–labeled ASC–CSM in a collagen gel matrix. (**G**) Bright field image of ASC-loaded CSM embedded in collagen gel, (**H**) epifluorescence image of CSM and migration of ASC into collagen matrix. White arrows show Qdot labeled ASC. (**I**) Overlay of epifluorescence image on bright field image of ASC in CSM (indicated by asterisks) and ASC in collagen gel (indicated by arrows), (**J**) immunofluorescence image of ASC in the collagen gel stained for Stro-1; white arrows indicate colocalization of Stro-1 and quantum dot 565–positive staining ASC. Color images available online at www.liebertonline.com/ten.

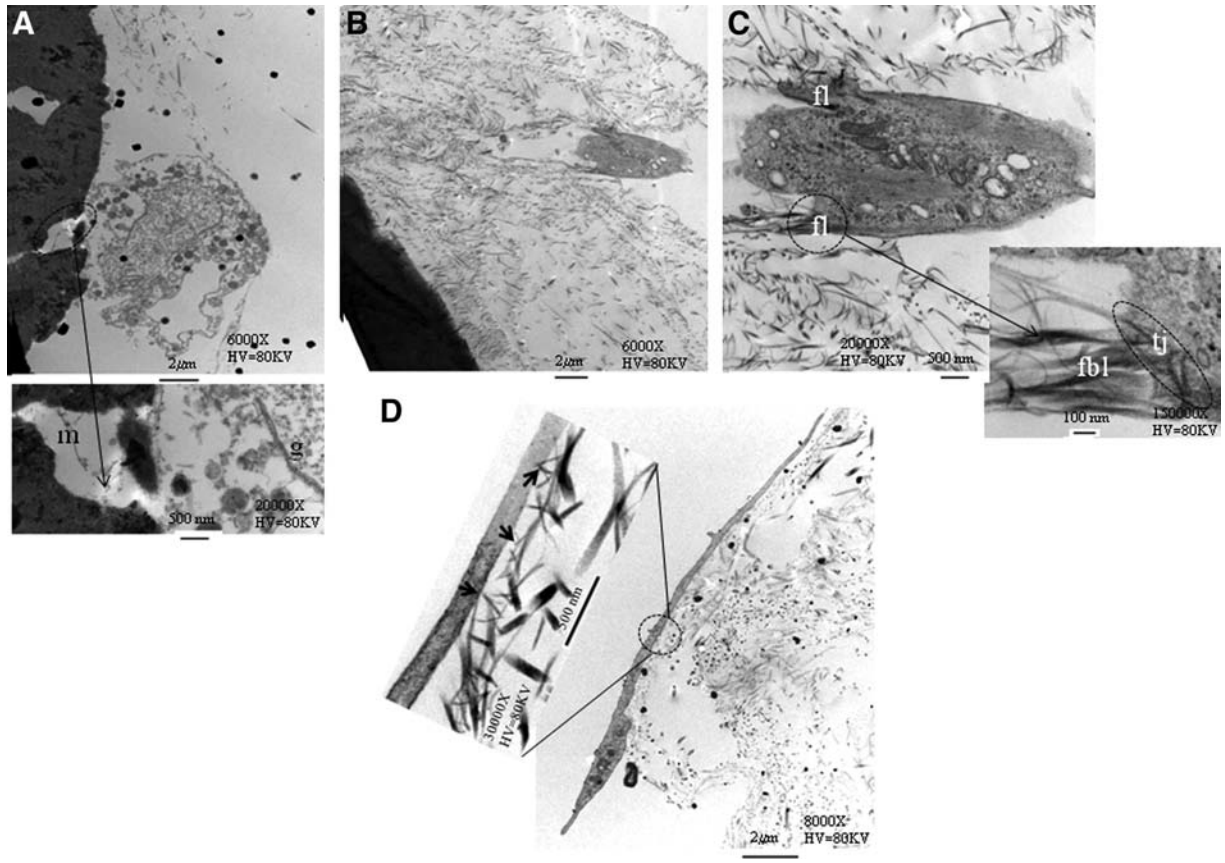

FIG. 11. Transmission electron microscopic images of ASC–CSM in collagen gel matrix. (**A**) Cell detaching from the CSM; (**A,** inset) the remaining attachment point to CSM (m) crevices during release into the surrounding collagen gel (g). (**B**) ASC that have migrated from CSM in the collagen matrix. (**C**) Higher magnification of ASC filopodias (fl) and attachment to collagen fibrils. Inset image shows the adhesion region of the cells to fibrils. (**D**) ASC that migrated into collagen gel (day 14) have elongated striated morphology and attach to collagen fibers (bold arrows) by forming nascent tight junction (tj).

the microspheres (inset of Figure 11A), round-up, and start to migrate away from the CSM and into the collagen gel (Figure 11B). Cells that have migrated into the gel form focal adhesions that appear as bundles of thin filaments located along the migration path with numerous collagen fibrils contacting the angled filopodia (Fig. 11C). The inset of Figure 11C shows the zone of adhesion between cells and collagen fibrils with possible formation of nascent tight junction (Fig. 11C). At day 14 cells can be found with a striated morphology and aligned along the matrix network, with its mature lamellipodia spanning over the collagen fibril for up to 12 μm (Fig. 11D) creating multiple focal adhesion points through minor spikes (inset, arrow heads).

ASC that have migrated out from CSM into collagen gel exhibit adipogenic differentiation

ASC that had migrated into collagen gel were induced to differentiate into adipocytes with adipogenic medium and stained with Oil Red O. As seen previously, the cells migrate throughout the collagen gel, when stained both the cells that on the surface of the gel (Fig. 12A) and inside the matrix (Fig. 12B) showed significant accumulation of oil droplets. In Figure 12B, the black arrows indicate Oil Red O–stained cells on different focal planes indicating that ASC have migrated completely throughout the collagen gel matrix.

Discussion

One of the major challenges in stem-cell-based therapy is the delivery of viable cells to the site of injury. The actual percentage of stem cells that can integrate and communicate with host cellular and ECM components is critically dependent on the carriers used and method to deliver. Biomaterial scaffolds are designed depending on the implantation type and site, with their material properties varying in chemical composition, mechanical strength, cellular response, and the overall 3D architecture.[52] An ideal biomaterial should provide favorable microenvironment for cells to attach and proliferate, while preserving their cell phenotype during *in vivo* transplantation.

In this study, CSM are used as a carrier device for adipose-derived stem cells. The specific ionic crosslinking methods used to prepare the microspheres resulted in greater than 90% of the spheres being within the size range of 175–225 μm. After crosslinking, the microspheres remain positively charged by retaining more than 98% of amino groups intact and are devoid of any major structural modifications in the chitosan polysaccharide chains. We have previously shown that high electropositivity of chitosan is beneficial for inducing cell migration and proliferation and is essential for chitosan–cell interaction *in vitro*.[45] The importance of the overall positive charge of chitosan has been confirmed in a recent report

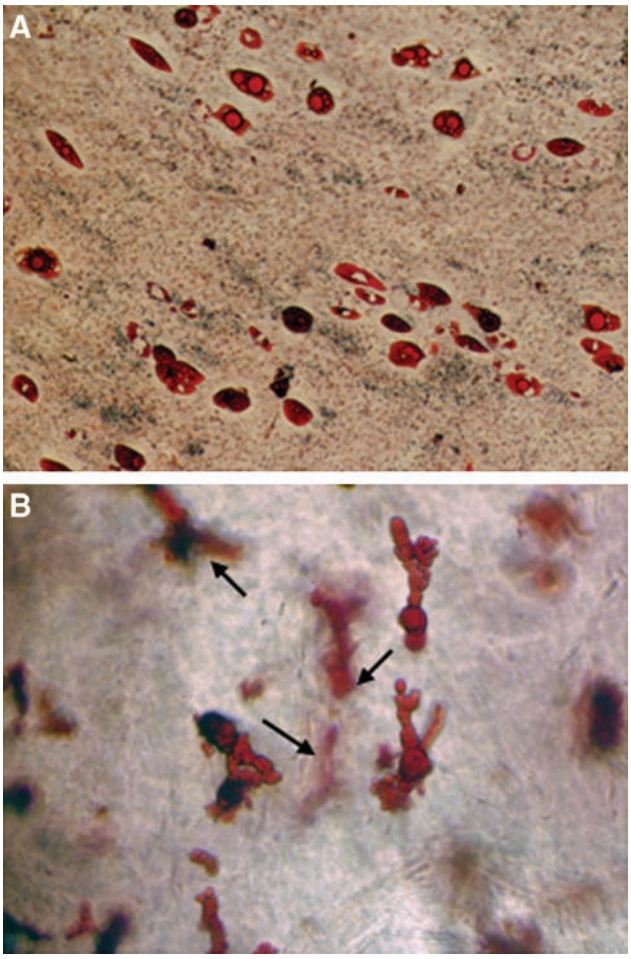

FIG. 12. Oil Red O staining of differentiated (day 24) ASC migrated from CSM in a collagen gel matrix. (**A**) Cells on the surface of the collagen gel and (**B**) cells that are present within the matrix. Black arrows point to differentiated cells on different focal planes, indicating that ASC have migrated throughout the collagen gel matrix. Color images available online at www.liebertonline.com/ten.

showing that chitosan-coated alginate microbeads increase adhesion of bone-marrow-derived stem cells and promote proliferation.[53]

In our cell loading experiments we validated the concept of an ideal cell-to-microsphere ratio and incubation time in terms of initial cell seeding density to achieve maximum number of cells that can be loaded in CSM. In our results of ACS loading onto the CSM it was observed that the percentage of cells on the CSM did not increase significantly beyond 48 h (Fig. 2A). The cells that did not attach to the CSM and remained on the cell culture inserts increased over 96 h irrespective of the initial cell loading (Fig. 2B). This increase in cell number can be attributed to ASC proliferation on the insert, which for higher seeding densities reached a plateau at 72 h. Therefore, it can be concluded that cell loading is maximized between 24 and 48 h; that there is a maximum cell loading capacity of the CSM, approximately 30,000 ASC per 5 mg CSM; and that cell proliferation of ASC is not inhibited by the CSM. Therefore, these parameters dictated the cell seeding density for our further studies involving the characterization of the release and differentiation of ASC from CSM *in vitro*, as well as the use of ASC-loaded CSM in collagen gel matrices, a key step for successful delivery *in vivo*.

In our *in vitro* culture insert system, the adipose stem cells use the CSM as an anchoring surface enabling a large number of cells to exist in a very small volume. Ultrastructural examination of cultured ASC with CSM shows that the ASC on the surface had elongated filopodia and a relatively flat and spindle-shaped morphology when compared to cells that had entered the crevices of the microsphere pores. We speculate that ASC retract their extended filopodia to get inside the matrix, as observed in TEM images (Figs. 4 and 5). When the ASC-loaded microspheres are plated into a larger area, the cells were able to migrate out of sphere. The migrated cells initially form small colonies around the microspheres (Fig. 3) and then proliferate eventually form a monolayer.

To determine whether the ASC that attach to the CSM retain their stem cell phenotype after they migrate from the microspheres, immunocytochemistry and FACS analysis were performed. Fluorescent photomicrographs comparing expression of stem-cell-specific markers (CD49d, CD54, CD71, CD90, Stro-1, and Sca-1) showed that control ASC and ASC that had migrated from the CSM express these markers in approximately the same amount and in the cellular distribution (Fig. 4A, B). Additionally, both ASC populations were negative for CD106 expression (data not shown), revealing the nonhematopoietic lineage of the cells.[43] FACS analysis of the cell populations from control ASC to the ASC that had migrated out of the CSM showed that the percentages of cells positive for CD54, CD90, and Stro-1 were very similar. These results are consistent with the earlier studies showing that these stem cell markers were present in adipose-derived stem cells and tissue.[51,54,55] In our FACS analysis the percentage of cells that express CD71 was significantly higher in the ASC cell population that migrated from the CSM, which may indicate a selective migration and/or expansion of a subpopulation of ASC under these conditions. This phenomenon may be attributed to the microsphere surfaces, as a recent study provides evidence that microcavities on scaffold surfaces improve cell adhesion and elicit differential cellular response in comparison to smooth surfaces.[56]

From the RT-PCR experiments (Fig. 8) it is evident that the chitosan microenvironment did not affect gene expression of stem-cell-specific markers, as the ASC that had migrated from CSM show relatively similar expression levels of stem-cell-specific genes when compared to control ASC cells. This indicates that the ASC that had migrated from the CSM maintain their stem cell phenotype.

Moreover, ASC that had migrated from the microspheres maintain their ability to differentiate into adipocytes and osteoblasts (Fig. 9). Notably, the migrated ASC showed a more intense lipid and calcium deposition than control ASC (passage 3) when stained with Oil Red O and Alizarin Red S dyes, respectively. Additionally, RT-PCR analysis revealed relatively higher expression level of leptin (11.7-fold) than the control ASC, which may be a contributing factor to increased levels of oil accumulation and hence more intense Oil Red O staining of the ASC from CSM. These results are consistent with the previous finding that lipid-filled processed lipoaspirate cells have increased expression levels of leptin.[43] When differentiated into osteoblasts, ASC from CSM showed a 6.2-fold higher expression level of ALP than the control ASC, which may have resulted in more intense Alizarin Red S

staining. Previously, it has been shown that increased levels of ALP expression significantly increase calcium deposition and that ALP is considered a key end differentiation marker.[43,57] Expression levels of other osteogenic-specific genes were found to be relatively close to the differentiated passage 3 ASC. This increase in end differentiation-specific markers (leptin in case of adipogenesis and ALP in for osteogenesis) indicates that most of the ASC that migrated from the CSM were multipotent and retained their ability to differentiate. This phenomenon may be attributed to the microsphere surfaces as a recent study provides evidence that microcavities on scaffold surfaces improve cell adhesion and elicit differential cellular response in comparison to smooth surfaces.[56] Further, micropores have been shown to increase the levels of BMP-2 and ALP, supporting dynamic osteogenic response of stem cells.[56] As structural aspects of scaffolds have been shown to be critical modulatory tool for the transcriptional regulation of gene expression in some cell types (e.g., osteoblasts and chondrocytes),[58] evaluation of structural attribution toward cell attachment and differentiation is pivotal in developing successful stem-cell-based tissue engineering therapies.

Finally, the successful delivery of stem cells from CSM into a 3D scaffolding architecture was accomplished in collagen gel matrix. Although site-specific delivery of stem cells using a microcarrier system was our primary goal, we also showed successful integration of ASC from the CSM into a 3D matrix. This was evaluated *in vitro* utilizing collagen gel to mimic *in vivo* conditions.

In our initial studies we showed that ASC could migrate from the microspheres onto a plastic culture surfaces, and that it is important to determine the usefulness of this system in a 3D environment. Previously, it has been shown that stem cells induce matrix contraction with a low concentration of collagen.[59] To avoid matrix contraction, we have used a high concentration of collagen to validate whether the cells could still migrate and proliferate into the surrounding ECM environment. Therefore, we added the ASC-loaded CSM to a collagen-based matrix that provided a stiffer 3D extracellular microenvironment. The cells adapted a unique morphology (Fig. 11) that can be attributed to the physical stiffness and molecular architecture of the collagen. It was evident from morphological evaluation that ASC migrate by extending their filopodias and pulling against the matrix (Fig. 11). Over time, the cells exhibited an elongated morphological structure forming characteristic focal adhesion points with multiple collagen microfibrils associated along with tight junctions resembling cells that are associated with stromal tissues.

Commitment of ASC to specific cell lineage was achieved by fine tuning the matrix stiffness and molecular architectures, analogous to a recent study providing evidence that stiffer gel induces mesenchymal cells to adopt a long striated or spindle-shaped morphology.[59] In our study ASC loaded in CSM were able to migrate and proliferate in collagen over time (Fig. 10) and still retained stem cell phenotype by staining positive for Stro-1 and colocalizing with Qdot 565 labeling (Fig. 10J).

When these migrated ASC in the collagen matrix were induced with adipogenic medium, they were able to differentiate into adipocytes and showed positive staining with Oil Red O. Cells that migrated to the surface of the gel differentiated with accumulation of oil droplet had linearly dispersed along the cytoplasm, and these are more close to type of morphology of the differentiated in a cell culture dish, whereas differentiated cells that had migrated deep into the gel matrix had unique 3D pattern of oil droplets, showing that ASC differentiation and lipid droplet formation was being influenced by the surrounding microenvironment. Further, by this study it is proposed that preconditioning cells in a 3D scaffold closely mimicking an ECM morphology would enable the ASC to differentiate into the intended cell morphology *in vivo*.

Conclusion

This investigation provides a new method to load ASC onto CSM, and illustrates that cells in the spheres can migrate while preserving their stemness. The porous CSM described provide an excellent microenvironment for ASC attachment and nutritional transport, allowing the cells to migrate into the spheres rather than being physically encapsulated as with other procedures. Immunophenotypic characterization provides evidence that ASC migrated out of CSM were true stem cells and method obviates the loss of vital cell-surface molecules, maintaining their phenotype within the microsphere environment. ASC could be successfully delivered into collagen matrix and can be induced to specifically differentiate into adipocytes, suggesting that ASC-loaded microspheres may be incorporated with suitable scaffolding architecture to develop specific tissue-engineered constructs. CSM can also be embedded in specific regions of scaffold to develop cell-patterned 3D architecture mimicking complex tissue structures. Further investigations to load other stem cell types and differentiated adult cells may provide the possibility to develop a tissue-engineered construct for a multicellular organ.

Acknowledgments

The authors would like to thank Ms. Janet Roe for isolation of adipose tissue and technical support. S.N. was supported by a Postdoctoral Fellowship Grant from the Pittsburgh Tissue Engineering Initiative. Confocal images were generated in the core optical imaging facility, which is supported by the University of Texas Health Science Center, San Antonio, TX, NIH-NCI P30 CA54174 (San Antonio Cancer Institute), NIH-NIA P30 AG013319 (Nathan Shock Center, San Antonio, TX), and NIH-NIA P01AG19316. The authors also thank Dr. Robert Reddick, Medical Director, and Lauren Chesnut, Technical Director, Electron Microscopy Facility, Department of Pathology, the University of Texas Health Science Center, San Antonio, TX, for use of facility and assistance in the analysis of electron micrographs.

Disclaimer

The opinions or assertions contained herein are the private views of the authors and are not to be construed as official or reflecting the views of the Department of Defense or U.S. Government. The authors are employees of the U.S. Government and this work was prepared as part of their official duties. All work was supported by U.S. Army Medical Research and Material Command.

Disclosure Statement

No competing financial interests exist.

References

1. Gimble, J.M., Katz, A.J., and Bunnell, B.A. Adipose-derived stem cells for regenerative medicine. Circ Res **100,** 1249, 2007.
2. Pountos, I., Corscadden, D., Emery, P., and Giannoudis, P,V. Mesenchymal stem cell tissue engineering: techniques for isolation, expansion and application. Injury **38(Suppl 4),** S23, 2007.
3. Tuan, R.S., Boland, G., and Tuli, R. Adult mesenchymal stem cells and cell-based engineering. Arthritis Res Ther **5,** 32, 2003.
4. Sylvester, K.G., and Loganker, M.T. Stem cells. Arch Surg **139,** 93, 2004.
5. Romanov, Y.A., Darevskaya, A.N., Merzlikina, N.V., and Buravkova, L.B. Mesenchymal stem cells from human bone marrow and adipose tissue: isolation, characterization, and differentiation potentialities. Bull Exp Biol Med **140,** 138, 2005.
6. Zuk, P.A., Zhu, M., Mizuno, H., Huang, J., Futrell, J.W., Katz, A.J, Benhaim, P., Lorenz, H.P., and Hedrick, M.H. Multilineage cells from human adipose tissue: implications for cell-based therapies. Tissue Eng **7,** 211, 2001.
7. Planat-Bernard, V., Silvestre, J.S., Cousin, B., Andre, M., Nibbelink, M., Tamarat, R., Clergue, M., Manneville, C., Saillan-Barreau, C., Durez, M., Tedgui, A., Levy, B., Penicaud, L., and Casteilla, L. Plasticity of human adipose lineage cells towards endothelial cells: physiological and therapeutic perspectives. Circulation **109,** 656, 2004.
8. Sgodda, M., Aurich, H., Kleist, S., Aurich, I., Konig, S., Dollinger, M.M., Fleig, W.E., and Christ, B. Hepatocyte differentiation of mesenchymal stem cells from rat peritoneal adipose tissue *in vitro* and *in vivo*. Exp Cell Res **313,** 2875, 2007.
9. Brzoska, M., Geiger, H., Gauer, S., and Baer, P. Epithelial differentiation of human adipose tissue-derived adult stem cells. Biochem Biophys Res Commun **330,** 142, 2005.
10. Aust, L., Devlin, B., Foster, S.J., Halvorsen, Y.D., Hicok, D., Du Laney, T., Sen, A., Willingmyre, G.D., and Gimble, J.M. Yield of human adipose-derived adult stem cells from liposuction aspirates. Cytotherapy **6,** 7, 2004.
11. McIntosh, K., Zvonic, S., Garrett, S., Mitchell, J.B, Floyd, Z.E., Hammill, L., Kloster, A., Di Halvorsen, Y., Ting, J.P., Storms, R.W., Goh, B., Kilroy, G., Wu, X., and Gimble, J.M. The immunogenicity of human adipose-derived cells: temporal changes *in vitro*. Stem Cells **24,** 1246, 2006.
12. Arnalich-Montiel, F., Pastor, S., Blazquez-Martinez, A., Fernandez-Delgado, J., Nistal, M., Alio, J.L., and De Miguel, M.P. Adipose-derived stem cells are a source for cell therapy of the corneal stroma. Stem Cells **26,** 570, 2008.
13. Puissant, B., Barreau, C., Bourin, P., Clavel, C., Corre, J., Bousquet, C., Taureau, C., Cousin, B., Abbal, M., Laharrague, P., Penicaud, L., Casteilla, L., and Blancher, A. Immunomodulatory effect of human adipose tissue-derived adult stem cells: comparison with bone marrow mesenchymal stem cells. Br J Haematol **129,** 118, 2005.
14. Cui, L., Yin, S., Liu, W., Li, N., Zhang, W., and Cao, Y. Expanded adipose-derived stem cells suppress mixed lymphocyte reaction by secretion of prostaglandin E2. Tissue Eng **13,** 1185, 2007.
15. Yanez, R., Lamana, M.L., Garcia-Castro, J., Colmenero, I., Ramirez, M., and Bueren, J.A. Adipose tissue-derived mesenchymal stem cells have *in vivo* immunosuppressive properties applicable for the control of the graft-versus-host disease. Stem Cells **24,** 2582, 2006.
16. Nakagami, H., Maeda, K., Morishita, R., Iguchi, S., Nishikawa, T., Takami, Y., Kikuchi, Y., Saito, Y., Tamai, K., Ogihara, T., and Kaneda, Y. Novel autologous cell therapy in ischemic limb disease through growth factor secretion by cultured adipose tissue derived stromal cells. Arterioscler Thromb Vasc Biol **25,** 2542, 2005.
17. Kim, W.S., Park, B.S., Sung, J.H., Yang, J.M., Park, S.B., Kwak, S.J., and Park, J.S. Wound healing effect of adipose-derived stem cells: a critical role of secretory factors on human dermal fibroblasts. J Dermatol Sci **48,** 15, 2007.
18. Zaragosi, L.-E., Ailhaud, G., and Dani, C. Autocrine fibroblast growth factor 2 signaling is critical for self-renewal of human multipotent adipose-derived stem cell. Stem Cells **24,** 2412, 2006.
19. Kang, S.K., Jun, E.S., Bae, Y.C., and Jung, J.S. Interactions between human adipose stromal cells and mouse neural stem cells *in vitro*. Brain Res Dev Brain Res **145,** 141, 2003.
20. Wang, B., Han, J., Gao, Y., Xiao, Z., Chen, B., Wang, X., Zhao, W., and Dai, J. The differentiation of rat adipose-derived stem cells into OEC-like cells on collagen scaffolds by co-culturing with OECs. Neurosci Lett **421,** 191, 2007.
21. Pountos, I., and Giannoudis, P.V. Biology of mesenchymal stem cells. Injury **36(Suppl 3),** S8, 2005.
22. Patrick, C.W. Tissue engineering strategies for adipose tissue repair. Anat Rec **263,** 361, 2001.
23. Krampera, M., Pizzolo, P., Aprili, G., and Franchini, M. Mesenchymal stem cells for bone, cartilage, tendon and skeletal muscle repair. Bone **39,** 678, 2006.
24. Zhang, D.Z., Gaim L.Y., Liu, H.W., Jin, Q.H., Huang, J.H., and Zhu, X.Y. Transplantation of autologous adipose-derived stem cells ameliorates cardiac function in rabbits with myocardial infarction. Chin Med J **120,** 300, 2007.
25. Tobita, M., Uysal, A.C., Ogawa, R., Hyakusoku, H., and Mizuno, H. Periodontal tissue regeneration with adipose-derived stem cells. Tissue Eng **14,** 945, 2008.
26. Barrilleaux, B., Phinney, D.G., Prokop, D.J., and O'Connor, K.C. Review: *ex vivo* engineering of living tissues with adult stem cells. Tissue Eng **12,** 3007, 2006.
27. Owens, B.D., Wenke J.C., Svoboda, S.J., and White, D.W. Extremity trauma research in United States Army. J Am Acad Orthop Surg **14(Suppl 10),** S37, 2006.
28. Chai, C., and Leong, K.W. Biomaterials approach to expand and direct differentiation of stem cells. Mol Ther **15,** 467, 2007.
29. Eslaminejad, M.B., Mirzadeh, H., Nickmahzar, A., Mohamadi, Y., and Mivehchi, H. Type I collagen gel in seeding medium improves murine mesencymal stem cell loading onto the scaffold, increases their subsequent proliferation, and enhances culture mineralization. J Biomed Mater Res B Appl Biomater **90,** 659, 2009.
30. Ma, K., Laco, F., Ramakrishna, S., Liao, S., and Chan, C.K. Differentiation of bone marrow-derivedmesenchymal stem cells into multi-layered epidermis-like cells in 3D organotypic coculture. Biomaterials **30,** 3251, 2009.
31. Lode, A., Bernhardt, A., and Gelinsky, M. Cultivation of human bone marrow stromal cells on three-dimensional scaffolds of mineralized collagen: influence of seeding density on colonization, proliferation and osteogenic differentiation. J Tissue Eng Regen Med **2,** 400, 2008.
32. Möllers, S., Heschel, I., Damink, L.H., Schügner, F., Deumens, R., Müller, B., Bozkurt, A., Nava, J.G., Noth, J., and Brook, G.A. Cytocompatibility of a novel, longitudinally microstructured collagen scaffold intended for nerve tissue repair. Tissue Eng Part A **15,** 461, 2009.

33. Mano, J.F., Silva, G.A., Azevedo, H.S., Malafaya, P.B., Sousa, R.A., Silva, S.S., Boesel, L.F., Oliveira, J.M., Santos, T.C., Marques, A.P., Neves, N.M., and Reis, R.L. Natural origin biodegradable systems in tissue engineering and regenerative medicine: present status and some moving trends. JR Soc Interface **4,** 999, 2007.
34. Chan, B.P., Hui, T.Y., Yeung, C.W., Li, J., Mo, I., and Chan, G.C.F. Self-assembled collagen-mesenchymal stem cell microspheres for regenerative medicine. Biomaterials **28,** 4652, 2007.
35. Herrero, E.P., Del Vale, E.M.M., and Galan, M.A. Immobilization of mesenchymal stem cells and monocytes in biocompatible microcapsules to cell therapy. Biotechnol Prog **23,** 940, 2007.
36. Gorodetsky, R., Clark, R.A.F., An, J., Gailit, J., Levdansky, L., Vexler, A., Berman, E., and Marx, G. Fibrin microbeads (FBM) as biodegradable carriers for culturing cells and for accelerating wound healing. J Invest Dermatol **112,** 866, 1999.
37. Ashton, R.S., Banerjee, A., Punyani, S., Schaffer, D.V., and Kane, R.S. Scaffolds based on degradable alginate hydrogels and poly(lactide-co-glycolide) microspheres for stem cell culture. Biomaterials **28,** 5518, 2007.
38. Na, K., Kim, S., Park, K., Kim, K., Woo, D.G., Kwon, I.C., Chung, H.M., and Park, K.H. Heparin/poly(l-lysine) nanoparticle-coated polymeric microspheres for stem-cell therapy. Am Chem Soc **129,** 5788, 2007.
39. Kim, I.Y., Seo, S.J., Moon, H.S., Yoo, M.K., Park, I.Y., Kim, B.C., and Cho, C.S. Chitosan and its derivatives for tissue engineering applications. Biotechnol Adv **26,** 1, 2008.
40. Shi, C., Zhu, Y., Ran, X., Wang, M., Su, Y., and Cheng, T. Therapeutic potential of chitosan and its derivatives in regenerative medicine. J Surg Res **133,** 185, 2006.
41. Zhu, Y., Liu, T., Song, K., Fan, X., Ma, X., and Cui, Z. *Ex vivo* expansion of adipose tissue-derived stem cells in spinner flasks. Biotechnol J **4,** 1198, 2009.
42. Altman, A.M., Yan, Y., Matthias, N., Bai, X., Rios, C., Mathur, A.B., Song, Y.H., and Alt, E.U. Human adipose-derived stem cells seeded on a silk fibroin-chitosan scaffold enhance wound repair in a murine soft tissue injury model. Stem Cells **27,** 250, 2009.
43. Zuk, P.A., Zhu, M., Ashjian, P., De Ugarte, D.A., Huang, J.I., Mizuno, H., Alfonso, Z.C., Fraser, J.K., Benhaim, P., and Hedrick, M.H. Human adipose tissue is a source of multipotent stem cells. Mol Biol Cell **13,** 4279, 2002.
44. Barthel, L.K., and Raymond, P.A. Improved method for obtaining 3-microns cryosections for immunocytochemistry. J Histochem Cytochem **38,** 1383, 1990.
45. Shanmuganathan, S., Shanmugasundaram, N., Adhirajanm, N., Ramyaa Lakshmi, T.S., and Babu, M. Preparation and characterization of chitosan microspheres for doxycycline delivery. Carbohydr Polym **73,** 201, 2008.
46. Bubins, W.A., and Ofner, C.M. The determination of (-amino groups in soluble and poorly soluble proteinaceous materials by a spectrophotometrie method using trinitrobenzenesulfonic acid. Anal Biochem **207,** 129, 1992.
47. Mosmann, T. Rapid colorimetric assay for cellular growth and survival: application to proliferation and cytotoxicity assays. J Immunol Methods **65,** 55, 1983.
48. Bornstein, M.B. Reconstituted rattail collagen used as substrate for tissue cultures on coverslips in Maximow slides and roller tubes. Lab Invest **7,** 134, 1958.
49. Chomczynski, P., and Sacchi, N. Single-step method of RNA isolation by acidguanidinium thiocyanate-phenol-chloroform extraction. Anal Biochem **162,** 156, 1987.
50. Livak, K.J., and Schmittgen, T.D. Analysis of relative gene expression data using real-time quantitative PCR and the 2(-Delta Delta C(T)) method. Methods **25,** 402, 2001.
51. Zannettino, A.C.W., Paton, S., Arthur, A., Khor, F., Itescu, S., Gimble, J.M., and Gronthos, S. Multipotent human adipose-derived stromal cells exhibit a perivascular phenotype *in vitro* and *in vivo*. J Cell Physiol **214,** 413, 2008.
52. Chai, C., and Leong, K.W. Biomaterials approach to expand and direct differentiation of stem cells. Mol Ther **15,** 467, 2007.
53. Wu, Y.-N., Yang, Z., Hui, J.H.P., Ouyang, H.-W., and Lee, E.H. Cartilagenous ECM component-modification of the micro-bead culture system for chondrogenic differentiation of mesenchymal stem cells. Biomaterials **28,** 4056, 2007.
54. Yamamoto, N., Akamatsu, H., Hasegawa, S., Yamada, T., Nakata, S., Ohkuma, M., Miyachi, E.-I., Marunouchim, T., and Matsunaga, K. Isolation of multipotent stem cells from mouse adipose tissue. J Dermatol Sci **48,** 43, 2007.
55. De Ugarte, D.A., Alfonso, Z., Zuk, P.A., Elbarbary, A., Zhu, M., Ashjian, P., Benhaim, P., Hedrick, M.H., and Fraser, J.K. Differential expression of stem cell mobilization-associated molecules on multi-lineage cells from adipose tissue and bone marrow. Immunol Lett **89,** 267, 2003.
56. Graziano, A., d'Aquino, R., Cusella-De Angelis, M.G., Laino, G., Piattelli, A., Pacifici, M., De Rosa, A., and Papaccio, G. Concave pit-containing scaffold surfaces improve stem cell-derived osteoblast performance and lead to significant bone tissue formation. PLoS ONE **2,** e496, 2007.
57. Rebelatto, C.K., Aguiar, A.M., Moretão, M.P., Senegaglia, A.C., Hansen, P., Barchiki, F., Oliveira, J., Martins, J., Kuligovski, C., Mansur, F., Christofis, A., Amaral, V.F., Brofman, P.S., Goldenberg, S., Nakao, L.S., and Correa, A. Dissimilar differentiation of mesenchymalstem cells from bone marrow, umbilical cord blood, and adipose tissue. Exp Biol Med (Maywood) **233,** 901, 2008.
58. Knippenberg, M., Helder, M.N., Doulabi, Z.B., Wuisman, P.I., and Klein-Nulend, J. Osteogenesis versus chondrogenesis by BMP-2 and BMP-7 in adipose stem cells. Biochem Biophys Res Commun **342,** 902, 2006.
59. Engler, A.J., Sen, S., Sweeney, H.L, and Discher, D.E. Matrix elasticity directs stem cell lineage specification. Cell **126,** 677, 2006.

Address correspondence to:
Robert J. Christy, Ph.D.
Regenerative Medicine Research Program
United States Army Institute of Surgical Research
3400 Rawley Chambers Ave., Building 3611
Fort Sam Houston, TX 78234-6315

E-mail: robert.christy@amedd.army.mil

Received: June 15, 2009
Accepted: November 16, 2009
Online Publication Date: February 17, 2010